Accelerating Airy wave packets in the presence of quadratic and cubic dispersion

Ioannis M. Besieris*
The Bradley Department of Electrical and Computer Engineering, Virginia Polytechnic Institute and State University, Blacksburg, Virginia 24060, USA

Amr M. Shaarawi
Physics Department, The American University of Cairo, P.O. Box 2511, Cairo 11511, Egypt

(Received 28 April 2008; published 10 October 2008)

The equation governing quadratic and cubic transparent dispersion within the framework of the slowly varying envelope approximation is shown to admit an infinite-energy uniformly moving Airy wave packet solution, as well as a square-integrable accelerating Airy solution. Some insight is provided regarding the local acceleration dynamics in the latter case and comparisons are made with the "accelerating" beam solution introduced by Siviloglou and Christodoulides and experimentally demonstrated by Siviloglou, Broky, Dogariu, and Christodoulides recently. It is shown, in particular, that under certain parametrizations, the presence of cubic dispersion can increase the "depth of penetration" of a wave packet. In other words, a pulse can propagate for a larger range without sustaining significant dispersive distortion than in the presence of quadratic dispersion alone. Finally, imaging properties of accelerating airy wave packets are discussed.

DOI: 10.1103/PhysRevE.78.046605 PACS number(s): 03.50.De, 41.20.Jb, 42.25.Bs, 42.25.Fx

I. INTRODUCTION

Electromagnetic wave propagation in a linear, homogeneous, transparent, dispersive medium is governed by the scalar equation

$$\nabla^2 u(\vec{r},t) + \beta_{op}^2(-i\partial/\partial t)u(\vec{r},t) = 0 \tag{1.1}$$

if polarization is neglected. In this expression, $u(\vec{r},t)$ is a real field and $\beta_{op}^2(-i\partial/\partial t)$ is a real pseudodifferential operator. A physical interpretation of the latter is provided in the frequency domain; specifically,

$$F\{\beta_{op}^2(-i\partial/\partial t)u(\vec{r},t)\} = \beta^2(\omega)\tilde{u}(\vec{r},\omega), \tag{1.2}$$

where $F\{\,\}$ denotes Fourier transformation and $\tilde{u}(\vec{r},\omega)$ is the Fourier transform of $u(\vec{r},t)$ with respect to time. The function $\beta(\omega)$ appearing on the right-hand side of Eq. (1.2) is a real wave number.

For a physically convenient central radian frequency ω_0, the real field $u(\vec{r},t)$ is expressed as follows:

$$u(\vec{r},t) = \psi(\vec{r},t)\exp[i\omega_0(t - z/v_{ph})] + cc, \quad z \geqslant 0. \tag{1.3}$$

Here, $\psi(\vec{r},t)$ is a complex-valued envelope function and $v_{ph} = \omega_0/\beta(\omega_0)$ denotes the phase speed in the medium computed at the central frequency ω_0. A formal introduction of Eq. (1.3) into Eq. (1.1) yields the following exact equation governing the envelope function $\psi(\vec{r},t)$:

$$\left[\nabla_\perp^2 + \frac{\partial^2}{\partial z^2} - 2i\beta(\omega_0)\frac{\partial}{\partial z} - \beta^2(\omega_0) + \sum_{m=0}^{\infty}\frac{1}{m!}\left.\frac{\partial^m}{\partial\omega^m}\beta^2(\omega)\right|_{\omega=\omega_0}\left(-i\frac{\partial}{\partial t}\right)^m\right]\psi(\vec{r},t) = 0. \tag{1.4}$$

Here, $\nabla_\perp^2$ denotes the transverse (with respect to z) Laplacian operator. Usually, at this stage in the study of wave propagation through dispersive media, one introduces the moving reference frame $\xi = z$, $\tau = t - (z/v_{gr})$, in terms of the group speed $v_{gr} = 1/\beta_1$; $\beta_1 \equiv d\beta(\omega)/d\omega|_{\omega=\omega_0}$. Then, Eq. (1.4) is transformed into

$$\left[\nabla_\perp^2 + \frac{\partial^2}{\partial z^2} + \frac{1}{v_{gr}^2}\frac{\partial^2}{\partial\tau^2} - 2\frac{1}{v_{gr}}\frac{\partial^2}{\partial z\partial\tau} - 2i\beta(\omega_0)\left(\frac{\partial}{\partial z} - \frac{1}{v_{gr}}\frac{\partial}{\partial\tau}\right) - \beta^2(\omega_0) + \sum_{m=0}^{\infty}\frac{1}{m!}\left.\frac{\partial^m}{\partial\omega^m}\beta^2(\omega)\right|_{\omega=\omega_0}\left(-i\frac{\partial}{\partial\tau}\right)^m\right]\psi(\vec{r},\tau) = 0. \tag{1.5}$$

A number of techniques have been developed based on the type of approximations made to the exact Eq. (1.5). In the sequel, use will be made of the *slowly varying envelope approximation* (SVEA) [1], whereby one neglects the second derivative with respect to z (paraxial approximation), as well as the mixed derivative term involving z and τ. Furthermore, dispersive effects up to third order will be retained. One, then, has

$$\left(i\frac{\partial}{\partial z} + \frac{1}{2}\beta_2\frac{\partial^2}{\partial\tau^2} + i\frac{B}{3}\frac{\partial^3}{\partial\tau^3}\right)\psi(\tau,z) = 0,$$

*besieris@vt.edu

$$B \equiv -\frac{1}{2\beta_0}\left(3\frac{\beta_2}{v_{gr}} + \beta_0\beta_3\right), \quad \beta_m \equiv d^m\beta(\omega)/d\,\omega^m\big|_{\omega=\omega_0}. \tag{1.6}$$

For normal dispersion, β_2 and B are positive and negative quantities, respectively. In this case, Eq. (1.6) can be nondimensionalized as

$$\left(i\frac{\partial}{\partial Z} + \frac{1}{2}\frac{\partial^2}{\partial T^2} - i\frac{b}{3}\frac{\partial^3}{\partial T^3}\right)\psi(T,Z) = 0, \quad T = \frac{\tau}{\tau_0}, \quad Z = z\frac{\beta_2}{\tau_0^2} \geqslant 0, \quad b = \frac{B}{\beta_2\tau_0} > 0, \tag{1.7}$$

where τ_0 is a convenient time scale. For anomalous dispersion, on the other hand, both β_2 and B are negative quantities. In this case, Eq. (1.6) can be nondimensionalized as

$$\left(i\frac{\partial}{\partial Z} - \frac{1}{2}\frac{\partial^2}{\partial T^2} + i\frac{b}{3}\frac{\partial^3}{\partial T^3}\right)\psi(T,Z) = 0, \quad T = \frac{\tau}{\tau_0}, \quad Z = -z\frac{\beta_2}{\tau_0^2} \geqslant 0, \quad b = \frac{B}{\beta_2\tau_0} > 0. \tag{1.8}$$

The discussion in the sequel will be restricted to the case of anomalous dispersion.

II. UNIFORMLY MOVING AIRY WAVE PACKET

The quadratic dispersion term in Eq. (1.8) can be eliminated by means of a gauge transformation [2]; specifically, through the new wave packet

$$\phi(T,Z) = \exp\left(i\frac{1}{2b}T\right)\exp\left(i\frac{1}{24b^2}Z\right)\psi\left(T + \frac{1}{4b}Z, Z\right), \tag{2.1}$$

which obeys the linearized Korteweg-deVries equation

$$\left(\frac{\partial}{\partial Z} + \frac{b}{3}\frac{\partial^3}{\partial T^3}\right)\phi(T,Z) = 0. \tag{2.2}$$

The latter has the following specific Airy solution:

$$\phi(T,Z) = \frac{1}{(bZ)^{1/3}}\mathrm{Ai}\left[\frac{T}{(bZ)^{1/3}}\right]. \tag{2.3}$$

(Of course, other solutions can be found by similarity methods.) The solution of Eq. (1.8) can be obtained by inverting Eq. (2.1) and using Eq. (2.3).

$$\psi(T,Z) = \frac{\exp\left[-i\frac{1}{24b^2}(a + 12bT - 2Z)\right]}{b^{1/3}(a+Z)^{1/3}}\mathrm{Ai}\left[\frac{T - Z/(4b)}{b^{1/3}(a+Z)^{1/3}}\right]. \tag{2.4}$$

In this expression, a is an arbitrary positive constant parameter. This non-square-integrable wave packet moves uniformly along the Z direction with an effective normalized speed equal to $4b$. This solution is clearly dispersive; it broadens in T as the range Z increases.

III. ACCELERATING AIRY WAVE PACKET

A general solution to Eq. (1.8) can be obtained by means of the Fourier synthesis

$$\psi(T,Z) = \int_{-\infty}^{\infty} d\Omega\, \exp(i\Omega T)\exp\left(i\frac{\Omega^2}{2}Z\right)\exp\left(ib\frac{\Omega^3}{3}Z\right)\tilde{\psi}_0(\Omega). \tag{3.1}$$

A specific solution arises from the modulated Gaussian spectrum

$$\tilde{\psi}_0(\Omega) = \exp(-a\Omega^2)\exp\left[\frac{i}{3}(\Omega^3 - 3a^2\Omega - ia^3)\right], \tag{3.2}$$

where a is a free positive parameter; specifically,

$$\psi(T,Z) = \frac{1}{(1+bZ)^{1/3}} \times\exp\left[\frac{6a(2T - Z^2) + iZ(-6a^2 - 6T + Z^2)}{12(1+bZ)^2}\right] \times\exp\left[b\frac{4Za(-a^2 + 3T + a^2bZ) + i6Z^2(a^2 - T)}{12(1+bZ)^2}\right] \times\mathrm{Ai}\left[\frac{\left(T - \frac{Z^2}{4} - iaZ\right) + bZ(T - a^2)}{(1+bZ)^{4/3}}\right]. \tag{3.3}$$

In the absence of cubic dispersion ($b=0$), this solution simplifies as follows:

$$\psi_{SC}(T,Z) = \exp\left[\frac{6a(2T - Z^2) + iZ(-6a^2 - 6T + Z^2)}{12}\right] \times\mathrm{Ai}\left(T - \frac{Z^2}{4} - iaZ\right). \tag{3.4}$$

This is essentially the analog of the finite-energy "accelerating" beam solution (for which the variable T is spacelike) introduced by Siviloglou and Christodoulides and experimentally demonstrated by Siviloglou, Broky, Dogariu, and Christodoulides recently [[3–5]; see also, Ref. [6]]. If, furthermore, the parameter a is set equal to zero, Eq. (3.4) becomes a variant of the infinite-energy (nonspreading) accelerating Airy solution to the one-dimensional Schrödinger equation introduced by Berry and Balazs [7] in the context of quantum mechanics, viz.,

$$\psi_{BB}(T,Z) = \exp\left[\frac{iZ(-6T + Z^2)}{12}\right]\mathrm{Ai}\left(T - \frac{Z^2}{4}\right). \tag{3.5}$$

It should be pointed out that $\psi_{SC}(T,Z)$ follows from the work in Appendix A of the Berry and Balazs paper [7]. Also, it can be derived from $\psi_{BB}(T,Z)$ in Eq. (3.5) through the complex translation $Z \to Z + i2a$ and the additional change $T \to T - a^2$.

Due to the infinite energy content of $\psi_{BB}(T,Z)$, the notions of a *centroid* (average temporal position) and *variance* (a measure of the average temporal pulse width or dispersive spreading in range) cannot be defined. This is not the case for the square-integrable solution $\psi(T,Z)$ given in Eq. (3.3). It is our aim to determine explicit expressions for these two av-

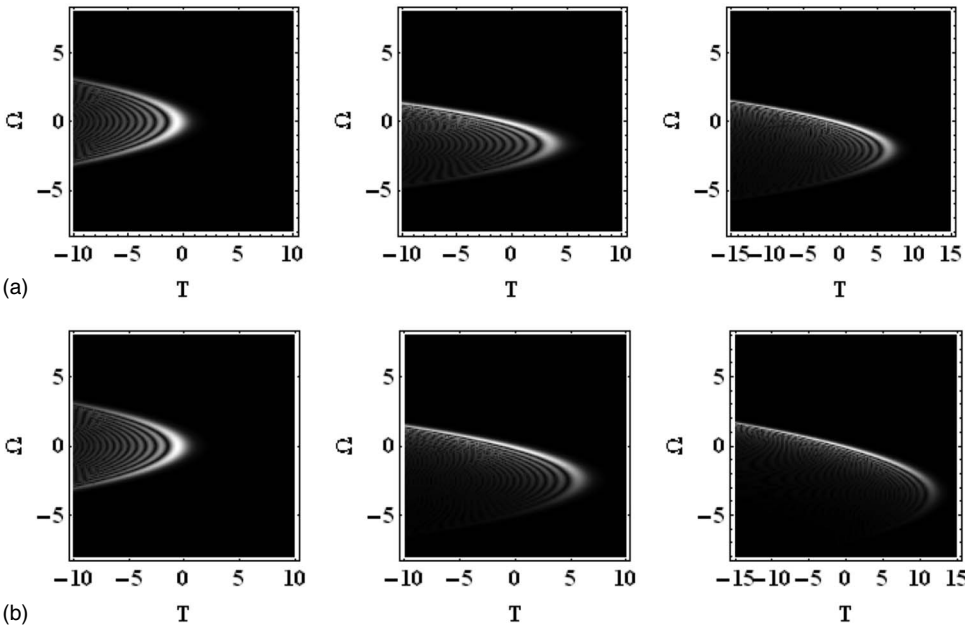

FIG. 1. (a) Density plot of the Wigner distribution function $W(T,\Omega,Z)$ vs T, Ω for three values of the normalized range Z: From left to right, $Z=0,5,7$. Parameter values: $a=5\times10^{-2}$, $b=10^{-1}$. (b) Density plot of the Wigner distribution function $W(T,\Omega,Z)$ vs T, Ω for three values of the normalized range Z: From left to right, $Z=0,5,7$. Parameter values: $a=5\times10^{-2}$, $b=0$.

eraged measures and use them to provide some insight regarding the nonlinear evolution of the wave packet. [The centroid and variance of the Siviloglou-Christodoulides solution $\psi_{SC}(T,Z)$ (see Ref. [6]) follow from those of $\psi(T,Z)$ in the limit as the parameter b becomes zero.]

It is convenient toward this goal to define first the phase-space (time-frequency) Wigner distribution, viz.,

$$W(T,\Omega,Z) \equiv \frac{1}{2\pi}\int_{-\infty}^{\infty} d\sigma \exp(i\sigma\Omega)\psi^*\left(T+\frac{1}{2}\sigma\right)\psi\left(T-\frac{1}{2}\sigma\right). \tag{3.6}$$

It can be determined explicitly as follows:

$$W(T,\Omega,Z) = \frac{1}{2^{1/3}\pi(1+bZ)^{1/3}}\exp\left\{\frac{2a\{3T(1+bZ)+Z[a^2b(-1+bZ)+3\Omega(1+bZ)]\}}{3(1+bZ)^2}\right\} \times \mathrm{Ai}\left\{\frac{2^{2/3}}{(1+bZ)^{4/3}}[T-a^2bZ+bTZ+\Omega(1+bZ)(Z+\Omega+bZ\Omega)]\right\}. \tag{3.7}$$

A comparison of the Wigner functions for $b\neq0$ and $b=0$ is shown in Figs. 1(a) and 1(b) for three values of the normalized range Z. The parameter values are $a=5\times10^{-2}$ in both figures, $b=10^{-1}$ for the first figure, and $b=0$ for the second one. The total energy and the desired centroid and variance can be obtained from the Fourier transform of $W(T,\Omega,Z)$ with respect to T, viz.,

$$\hat{W}(S,\Omega,Z) \equiv \int_{-\infty}^{\infty} dT \exp(iTS)W(T,\Omega,Z). \tag{3.8}$$

Specifically,

$$TE(\text{total energy}) = \int_{-\infty}^{\infty} d\Omega \hat{W}(0,\Omega,Z) = \frac{\exp(2a^3/3)}{4\pi^{3/2}\sqrt{2a}},$$

$$\langle T(Z)\rangle(\text{centroid}) = i\frac{1}{TE}\int_{-\infty}^{\infty} d\Omega \frac{\partial}{\partial S}\hat{W}(0,\Omega,Z) = \frac{1-4a^3+bZ}{4a},$$

$$\sigma^2(Z)(\text{variance}) = -\frac{1}{TE}\int_{-\infty}^{\infty} d\Omega \frac{\partial^2}{\partial S^2}\hat{W}(0,\Omega,Z) = \frac{8a^3+2aZ^2+(1+bZ)^2}{8a^2}. \tag{3.9}$$

Setting b equal to zero one obtains the corresponding averaged quantities for the Siviloglou-Christodoulides solution (see Ref. [6]) as follows:

$$TE_{SC} = \frac{\exp(2a^3/3)}{4\pi^{3/2}\sqrt{2a}},$$

$$\langle T(Z)\rangle_{SC} = \frac{1-4a^3}{4a},$$

$$\sigma^2(Z)_{SC} = \frac{8a^3 + 2aZ^2 + 1}{8a^2}. \tag{3.10}$$

It should be noted that both $\psi(T,Z)$ and $\psi_{SC}(T,Z)$ contain the same total energy and their variances change parabolically in range. However, the centroid of the former varies linearly in range whereas that of the latter is constant.

Being the square-integrable version of Eq. (3.5), the Siviloglou-Christodoulides accelerating Airy wave packet given in Eq. (3.4) has the property that it can propagate for long ranges Z without significant dispersive distortion as long as the positive parameter a is small (of the order of 10^{-2}). An important question, then, is the following: What is the effect of the third-order dispersion parameter b on the spreading properties of the Airy solution given in Eq. (3.3)? A composite of the graphs $|\psi(T,Z)|^2$ versus T (blue, light gray) and $|\psi_{SC}(T,Z)|^2$) versus T (red, dark gray) for different values of the normalized range Z is shown in Fig. 2. The parameter values are $a=5\times10^{-2}$ and $b=10^{-1}$ for Fig. 2(a) and $a=10^{-1}$ and $b=10^{-1}$ for Fig. 2(b). It is seen that the presence of cubic dispersion increases the "depth of penetration" of the wave packet. In other words, the pulse can propagate for a larger range without sustaining significant dispersive distortion than in the presence of quadratic dispersion only. This seems to be a surprising result because a comparison of the variances in Eqs. (3.9) and (3.10) shows that $\sigma^2(Z)$ increases faster with range than $\sigma^2(Z)_{SC}$. However, we use as a measure of the effectiveness of the accelerating Airy solution $\psi(T,Z)$ against dispersive distortion the integrity of its major lobe with range. It will be shown below that such an effectiveness arises from the different acceleration rates of $\psi(T,Z)$ and $\psi_{SC}(T,Z)$.

It is instructive to examine the local reshaping of the intensity $|\psi(T,Z)|^2$ as the range Z increases using the de Broglie-Bohm [8] approach, which has been proven very useful in quantum mechanics. Toward this end, the solution to Eq. (1.8) is written as

$$\psi(T,Z) = R(T,Z)\exp[iS(T,Z)], \tag{3.11}$$

where both the amplitude $R(T,Z)$ and the phase $S(T,Z)$ are real functions. Then, a family of local trajectories (rays) can be obtained by setting up the Hamilton-Jacobi equations

$$\frac{d}{dZ}T(Z) = v(Z), \quad \frac{d}{dZ}v(Z) = -\frac{\partial}{\partial T}Q(T,Z)|_{T\to T(Z)},$$

$$Q(T,Z) \equiv -\frac{1}{2R(T,Z)}\frac{\partial^2}{\partial T^2}R(T,Z). \tag{3.12}$$

The function $Q(T,Z)$ is known as the Bohm quantum mechanical potential when Z is timelike, as in the case of the $(1+1)D$ Schrödinger equation. An alternative method for establishing local trajectories is to use the de Broglie-Bohm method as follows:

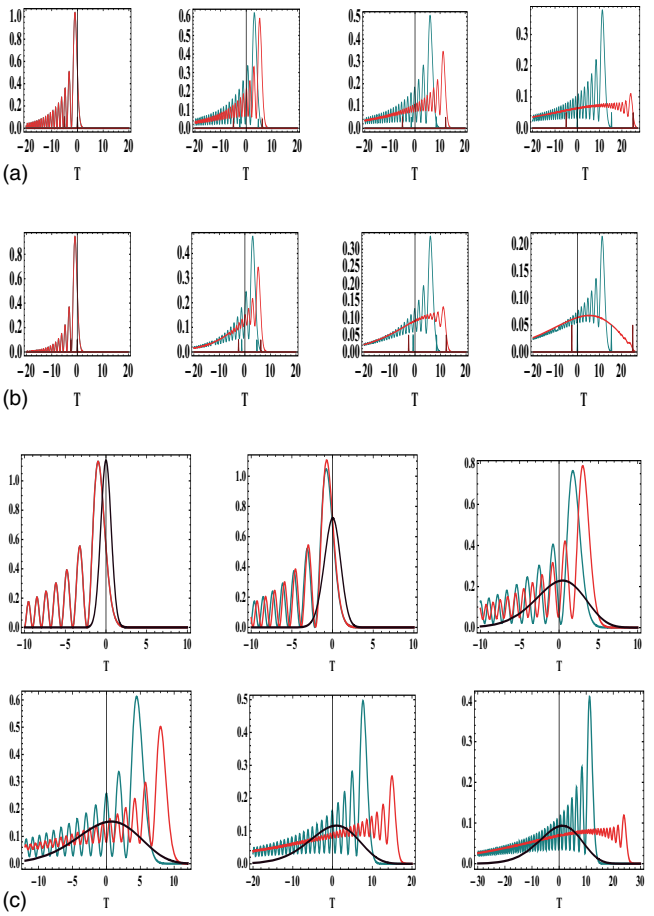

FIG. 2. (Color online) (a) Composite of the graphs $|\psi(T,Z)|^2$ vs T (blue, light gray), and $|\psi_{SC}(T,Z)|^2$ vs T (red, dark gray) for different values of the normalized range Z: From left to right, $Z=0,5,7,10$. Parameter values: $a=5\times10^{-2}$, $b=10^{-1}$. (b) Composite of the graphs $|\psi(T,Z)|^2$ vs T (blue, light gray), and $|\psi_{SC}(T,Z)|^2$ vs T (red, dark gray) for different values of the normalized range Z: From left to right, $Z=0,5,7,10$. Parameter values: $a=10^{-1}$, $b=10^{-1}$. (c) Composite of the graphs $|\psi(T,Z)|^2$ vs T (blue, light gray), $|\psi_{SC}(T,Z)|^2$ vs T (red, dark gray), and $|\psi_G(T,Z)|^2$ vs T (black) for different values of the normalized range Z: From left to right, $Z=0,1,4,6,8,10$. Parameter values: $a=5\times10^{-2}$, $b=10^{-1}$.

$$\frac{d}{dZ}T(Z) = v(Z),$$

$$v(Z) = \left[-\frac{\partial}{\partial T}S(T,Z) = \mathrm{Im}\left\{\frac{\psi^*(T,Z)(\partial/\partial T)\psi(T,Z)}{|\psi(T,Z)|^2}\right\}\right]_{T\to T(Z)}. \tag{3.13}$$

Let us first apply Eq. (3.12) or (3.13) to the infinite energy Berry-Balazs wave packet $\psi_{BB}(T,Z)$ given in Eq. (3.5). A straightforward calculation yields the relation $dT/dZ=Z/2$. One interpretation is that, *modulo* a constant assumed to equal zero, the rightmost lobe of the Airy wave packet $\psi_{BB}(T,Z)$ moves in range according to the formula $T=Z^2/4$, which precisely coincides with the expression obtained by setting the argument of the Airy function in Eq. (3.5) equal to zero.

If, next, the de Broglie–Bohm formalism is applied to the Siviloglou-Christodoulides wave packet $\psi_{SC}(T,Z)$ given in Eq. (3.4), one obtains

$$\frac{d}{dZ}T(Z) = \frac{Z}{2} + \mathrm{Im}\left\{\frac{\mathrm{Ai}'[-iaZ + T(Z) - Z^2/4]}{\mathrm{Ai}[-iaZ + T(Z) - Z^2/4]}\right\}, \tag{3.14}$$

where Ai′( ) denotes the derivative of the Airy function with respect to its argument. It is clearly seen in this case that the rightmost lobe of the Airy wave packet $\psi_{SC}(T,Z)$ evolves in range approximately according to the formula $T=Z^2/4$ only for very small values of the parameter a, as correctly pointed out in Ref. [3].

The de Broglie–Bohm formalism is applied finally to the wave packet $\psi(T,Z)$ given in Eq. (3.3), which arises from the presence of both quadratic and cubic dispersion. As a result, one obtains

$$\frac{d}{dZ}T(Z) = \frac{1}{2}\frac{Z}{1+bZ} + \mathrm{Im}\left\{\frac{\mathrm{Ai}'[T + bTZ - Z(4ia + 4a^2b + Z)/4]}{\mathrm{Ai}[T + bTZ - Z(4ia + 4a^2b + Z)/4]}\right\}. \tag{3.15}$$

In this case, the rightmost lobe of the Airy wave packet $\psi(T,Z)$ evolves in range approximately according to the formula $T=(Z/2b)-\ln(1+bZ)/2b^2$ for very small values of the parameter a. This behavior differs from the expression $T=(a^2bZ+Z^2/4)/(1+bZ)$ one would obtain by setting equal to zero the real part of the argument of the Airy function in Eq. (3.3). It should be noted that in the limit as b approaches zero (no cubic dispersion), both expressions above tend to $T=Z^2/4$. For a finite value of the parameter b, both expressions above tend to $T=Z^2/4$ for small values of the parameter a and the range Z. For larger ranges, the Siviloglou-Christodoulides wave packet accelerates faster than the solution $\psi(T,Z)$ associated with both quadratic and cubic dispersion. It is clear from Fig. 2 that it is this slowdown arising from the presence of cubic dispersion that adds to the depth of penetration of the wave packet. The differences in the variances mentioned earlier play a minor role. For the parameters used in Fig. 2(b), for example, the standard deviations of $\psi(T,Z)$ and $\psi_{SC}(T,Z)$ at $Z=10$ equal 8.6617 and 8.1024, respectively.

The ticks on the bottom of the graphs in Figs. 2(a) and 2(b) have the following meaning. Starting from the left side, the first and second ticks indicate the positions of the centroids of $\psi_{SC}(T,Z)$ and $\psi(T,Z)$, respectively. The third tick is the value $T=(Z/2b)-\ln(1+bZ)/2b^2$ corresponding to the approximate motion of the front of the major lobe of the wave packet $\psi(T,Z)$ for small values of the parameter a. The rightmost tick indicates the value $T=Z^2/4$ corresponding to the approximate motion of the major lobe of the wave function $\psi_{SC}(T,Z)$ for small values of the parameter a.

Consider, next, the normalized Gaussian pulse $\psi_0(T) = \exp[-T^2/(2\sigma^2)]/(\pi^{1/4}\sqrt{\sigma})$ at $Z=0$. This initial pulse evolves in a medium characterized by anomalous quadratic and cubic dispersion as follows:

$$\psi_G(T,Z) = \frac{\pi^{1/4}\sqrt{2\sigma}}{(bZ)^{1/3}}\exp\left\{\frac{(\sigma^2 - iZ)[6bTZ - (Z + i\sigma^2)]}{12b^2Z^2}\right\} \times \mathrm{Ai}\left[\frac{4bTZ - (Z + i\sigma^2)}{4(bZ)^{4/3}}\right]. \tag{3.16}$$

A superposition of Fig. 1(a) and the evolution of wave packet $\psi_G(T,Z)$ is shown in Fig. 2(c). The width of the initial Gaussian pulse has been chosen to be approximately the same with the widths of the main lobes of $\psi(T,Z)$ and $\psi_{SC}(T,Z)$ at $Z=0$. The parameters a and b are identical to those in Fig. 1(a). Figure 2(c) clearly shows the significant dispersive spreading of the Gaussian pulse in comparison to the dispersive spreading of the main lobes of both $\psi(T,Z)$ and $\psi_{SC}(T,Z)$. Of course, as already mentioned, the dispersive distortion of $\psi_{SC}(T,Z)$ is more pronounced than that of $\psi(T,Z)$.

IV. IMAGING WITH ACCELERATING AIRY WAVE PACKETS

It is desirable in some applications to synthesize the input signal at $Z=0$ so that the output signal has some optimal characteristics (e.g., pulse width) at some prescribed space-time point. In "chirped" radar systems, for example, the input signal is frequency modulated, which, in turn, gives rise to the phenomenon of pulse compression. An example of such pulse "imaging" in media characterized by both quadratic and cubic dispersion will be shown in this section using a special square-integrable initial condition.

For the solution of Eq. (1.8) to have the property of imaging, the spectrum $\tilde{\psi}_0(\Omega)$ in Eq. (3.1) is chosen as follows:

$$\tilde{\psi}_0(\Omega) = \Gamma\exp(-a\Omega^2)\exp\left(\frac{i}{3}p\Omega^3\right). \tag{4.1}$$

Here, p is a parameter *smaller than zero* that will determine the range $Z=|p|$ at which the initial condition will "image" to a desired pulse. Using the standard normalization constraint

$$\int_{-\infty}^{\infty} dT\psi_0^*(T)\psi_0(T) = 1, \tag{4.2}$$

Γ and a must satisfy the relation $a=\Gamma^4/(8\pi)$. Then, the initial pulse can be determined explicitly as follows:

$$\begin{aligned}\psi_0(T) &= \frac{1}{2\pi}\int_{-\infty}^{\infty} d\Omega\Gamma\exp(i\Omega T)\exp\left(ip\frac{\Omega^3}{3}\right)\exp(-a\Omega^2)\\ &= \frac{1}{2\pi}\int_{-\infty}^{\infty} d\Omega\Gamma\exp(-i\Omega T)\exp\left(i|p|\frac{\Omega^3}{3}\right)\exp(-a\Omega^2)\\ &= \frac{\Gamma}{|p|^{1/3}}\exp\left[-\frac{a(2a^2+3|p|T)}{3|p|^2}\right]\mathrm{Ai}\left(\frac{a^2}{|p|^{4/3}} - \frac{T}{|p|^{1/3}}\right).\end{aligned} \tag{4.3}$$

When the modified modulated Gaussian spectrum given in Eq. (4.1) is introduced into Eq. (3.1) three distinct cases must be considered.

Case (i). $Z+p<0$.

$$\psi_<(T,Z)=\frac{\Gamma}{|p+bZ|^{1/3}}\times\exp\left\{i(ia+Z/2)\left[\frac{2(ia+Z/2)^2}{3|p+bZ|^2}+\frac{T}{|p+bZ|}\right]\right\}\times\mathrm{Ai}\left[-\frac{(ia+Z/2)^2}{|p+bZ|^{4/3}}-\frac{T}{|p+bZ|^{4/3}}\right]. \tag{4.4}$$

Case (ii). $Z+p=0$.

$$\psi(T,Z=-p)=\frac{1}{\sqrt{2\pi}}\frac{\Gamma}{\sqrt{2a-i|p|}}\exp\left(-\frac{1}{2}\frac{T^2}{2a-i|p|}\right). \tag{4.5}$$

Case (iii). $Z+p>0$.

$$\psi_>(T,Z)=\frac{\Gamma}{|p+bZ|^{1/3}}\times\exp\left\{i(ia+Z/2)\left[\frac{2(ia+Z/2)^2}{3|p+bZ|^2}-\frac{T}{|p+bZ|}\right]\right\}\times\mathrm{Ai}\left[-\frac{(ia+Z/2)^2}{|p+bZ|^{4/3}}+\frac{T}{|p+bZ|^{4/3}}\right]. \tag{4.6}$$

For the problem under consideration, the solution "pivots" about $Z=-p$, where the "desired" Gaussian pulse is formed. The image range is seen to equal $Z=2|p|$. The evolution of $|\psi_<(T,Z)|^2$ from $Z=0$ to $Z=1$ is shown in Fig. 3(a) and the evolution of $|\psi_>(T,Z)|^2$ for $Z\geqslant 1$ is shown in Fig. 3(b) for the parameter values $a=10^{-1}$, $b=5\times10^{-1}$, and $p=-5\times10^{-1}$. The wavelets displaced away from the main pulse at $Z=0$ contain higher temporal frequencies than those close to the origin and, therefore, have larger velocities of propagation. For $0<Z<1$, these wavelets converge on the ones moving at smaller velocities. The imaging of the initial pulse to the Gaussian one at the range $Z=1$ is the result of this "dispersive focusing."

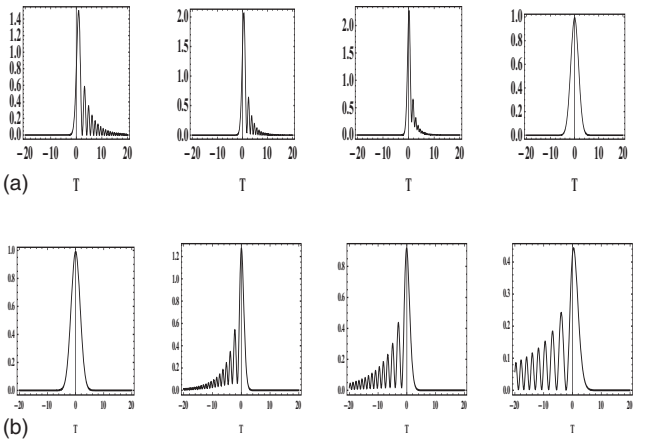

FIG. 3. (a) Evolution of $|\psi_<(T,Z)|^2$ vs T for four values of the normalized range Z: From left to right, $Z=0,0.5,0.7,1$. Parameter values: $a=10^{-1}$, $b=5\times10^{-1}$, $p=-5\times10^{-1}$. (b) Evolution of $|\psi_>(T,Z)|^2$ vs T for four values of the normalized range Z: From left to right, $Z=1,2,3,8$. Parameter values: $a=10^{-1}$, $b=5\times10^{-1}$, $p=-5\times10^{-1}$.

V. CONCLUDING REMARKS

It has been shown that the equation governing quadratic and cubic transparent dispersion within the framework of the slowly varying envelope approximation can admit infinite-energy uniformly moving Airy wave packet solutions as well as square-integrable accelerating Airy solutions. Some insight has been provided regarding the local acceleration dynamics in the latter case and comparisons have been made with the "accelerating" beam solutions introduced by Siviloglou and Christodoulides and experimentally demonstrated by Siviloglou, Broky, Dogariu, and Christodoulides recently. It has been shown that under particular parametrizations the presence of cubic dispersion can increase the "depth of penetration" of the wave packet. In other words, the pulse can propagate for a larger range without sustaining significant dispersive spreading than in the presence of quadratic dispersion alone. Finally, physically applicable imaging properties of accelerating Airy wave packets have been discussed.

[1] T. Brabec and F. Krausz, Phys. Rev. Lett. **78**, 3282 (1997).
[2] H. Wang, Electron. J. Differ. Equations **2007**, 1 (2007).
[3] G. A. Siviloglou and D. N. Christodoulides, Opt. Lett. **32**, 979 (2007).
[4] G. A. Siviloglou, J. Broky, A. Dogariu, and D. N. Christodoulides, Phys. Rev. Lett. **99**, 213901 (2007).
[5] G. A. Siviloglou, J. Broky, A. Dogariu, and D. N. Christodoulides, Opt. Lett. **33**, 207 (2008).
[6] I. M. Besieris and A. M. Shaarawi, Opt. Lett. **32**, 2447 (2007).
[7] M. V. Berry and N. L. Balazs, Am. J. Phys. **47**, 264 (1979).
[8] D. Bohm, Phys. Rev. **85**, 166 (1952).